Electronic Supplementary Material (ESI) for Physical Chemistry Chemical Physics
This journal is © The Owner Societies 2013

Electronic Supplementary Information

H-loop Histidine Catalyzes ATP Hydrolysis in the *E. coli* ABC Transporter HlyB

*Yan Zhou, Pedro Ojeda-May, and Jingzhi Pu**

Depart of Chemistry and Chemical Biology, Indiana University-Purdue University Indianapolis, Indianapolis, IN 46202

* To whom correspondence should be addressed. Email: jpu@iupui.edu

1. Schematic representation of hydrogen bonding interactions near the center of the active site in HlyB

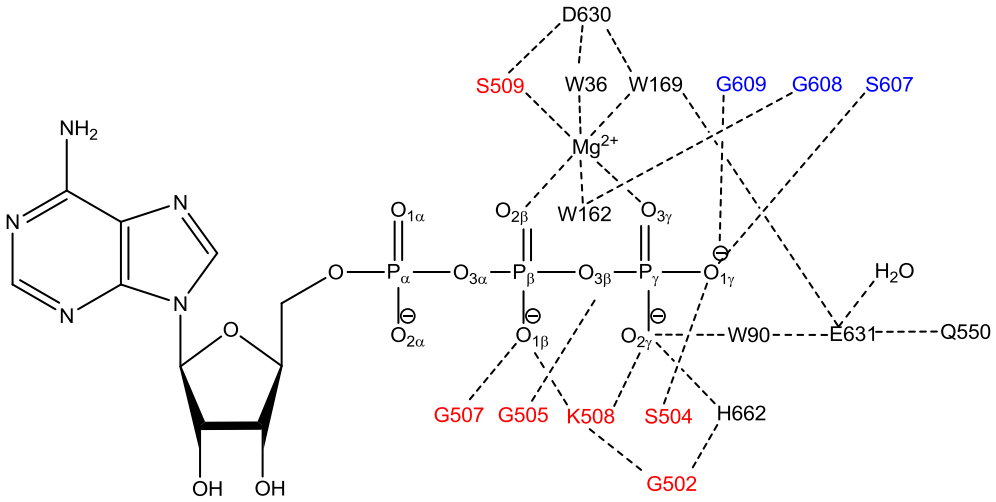

Scheme S1. Selected hydrogen bonding interactions in the active site of *E. coli* HlyB-NBDs. Residues in red are in the Walker A motif (or P-loop). Residues in blue are in the C-loop (or signature loop), which is from the opposite monomer. D630 is in the Walker B motif. E631 is near the end of Walker B. H662 is in the H-loop.

2. Details of building the simulation model by combing two HlyB structures.

The 1XEF structure contains ATP/Mg^{2+} bound HlyB-NBDs with H662A mutations. The 2FGK structure contains E631Q mutations of HlyB-NBDs bound with ATP in the absence of Mg^{2+}. The simulation system was built based on the NBD dimer in the 1XEF structure, except that the 2FGK structure was used to model H662, E631, and the lytic water (W_L) (Figure 1b in the main text). The modeling of E631 is necessary because its original orientation in the 1XEF structure is not suited to activate the lytic water. The unsuitable side chain orientation of E631 may be caused by the mutation at the position of H662A in 1XEF. In contrast, the side chain orientation of Q631 in 2FGK, although presented as a mutant of E631, adopts a position that better aligns W_L for an in line

Electronic Supplementary Material (ESI) for Physical Chemistry Chemical Physics
This journal is © The Owner Societies 2013

attack. Each of the two NBDs in the 2FGK structure contains a water molecule in the vicinity of P_γ of ATP, H662, and Q631. Thus the positions of these crystal water molecules in 2FGK were also used to model W_L in the 1XEF-based simulation system.

3. Justification of using the AM1/CHARMM method

The AM1 method is chosen here because of its stability, efficiency, and reasonable accuracy for the overall reaction energy based on the hydrolysis of methyl triphosphate (in the gas phase) as a model reaction (Pu *et al.*, unpublished). A reviewer asked why we did not use any specialized semiempirical method such as AM1/d-P (Lopez & York, *TCA* **2003**, *109*, 149) in our calculations. We did not choose these specialized methods, including AM1/d-P, AM1/d-PhoT (Nam *et al. JCTC* **2007**, *3*, 486), and SCC-DFTB-PR(PA) (Yang *et al. Phys. Chem. A* **2007**, 111, 10861), and AM1-SRP [Arantes & Loos *PCCP* **2006**, *8*, 347], mainly because they do not seem to provide parameters consistently obtained for N. Reliable parameters for N are important in the present study of the GAC mechanism that involves His-mediated proton transfers. The lack of N parameters (or the lack of validation of the mixed use of these specific reaction parameters with standard parameters on N) made it difficult to directly apply these specialized methods to our calculations. The AM1 method, on the other hand, provides consistent parameters on H, C, N, O, and P, and thus was chosen for its generality. The underlying assumption of this choice is that systematic errors (if any) associated with the AM1 Hamiltonian would largely cancel out in distinguishing the operative mechanisms from those non-operative ones, especially when the same simulation protocol is applied to the same enzyme configuration. Note that the comparison of the GAC and the SAC mechanism in elucidating H662's functional role is the main focus of the present work.

4. Detailed description of the system preparation for the QM/MM calculations and additional SHAKE constraints

The protons in the guanidinium group of K508 were also constrained by SHAKE during MD simulations and energy scans to avoid irrelevant proton transfers. In addition, H_N of H662 was constrained by SHAKE in the SAC mechanism.

5. Detailed discussions on geometries of stationary points for the GAC and the SAC mechanisms

5.1. Geometries and energetics of stationary points for the GAC mechanism

The PES of the GAC mechanism (Figure 2a) reveals a four-step process for ATP hydrolysis. Key geometric parameters and energetics of the stationary points determined for the GAC mechanism are listed in Table S1.

Electronic Supplementary Material (ESI) for Physical Chemistry Chemical Physics
This journal is © The Owner Societies 2013

Table S1. Bond distances, dihedral angles, and energies of stationary points in the GAC mechanism (Figure 2a).[a]

	RC1	RC2	Distance (Å)						$O_{1\gamma}$-P_γ-$O_{2\gamma}$-$O_{3\gamma}$ (degrees)	ΔE
			H_N-N_ε	H_N-$O_{2\gamma}$	H_W-O_W	H_W-N_ε	P_γ-$O_{3\beta}$	P_γ-O_W		
Min1	-3.60	-2.10	1.00	2.07	0.97	3.49	1.65	3.75	146	-2.4
TS1	-2.90	-1.19	1.00	2.04	0.96	2.82	1.65	2.85	150	9.0
Min2	-3.00	-0.30	1.01	1.93	0.97	3.05	1.70	2.00	160	0.0
TS2	-1.81	-0.30	1.11	1.47	0.99	2.44	1.71	2.01	162	15.0
Min3	-1.20	-0.30	1.87	0.97	0.96	3.06	1.65	1.94	161	5.6
TS3	2.30	0.29	3.68	0.95	1.11	1.54	2.02	1.72	-169	22.1
Min4	3.40	0.30	3.24	0.95	2.11	1.00	1.93	1.63	-163	-9.2
TS4	3.40	1.50	3.34	0.96	2.03	1.00	3.09	1.59	-134	4.7
Min5	3.40	1.70	3.34	0.96	2.03	1.01	3.29	1.59	-131	3.1

[a]Distances are in Å, dihedral angles in degrees, and energies in kcal/mol.

In the first step of the calculated GAC mechanism, the catalytic water approaches ATP to form a reactant complex Min1. The second step of the GAC mechanism is a proton transfer from H662 to the electronegative $O_{2\gamma}$ of ATP with a barrier height of 15.0 kcal/mol (TS2). The energy of the resulting intermediate (Min3) is 5.6 kcal/mol relative to the reactant state (Min2). Hydrogen bonding interactions involving the imidazolate ion in Min3 include a bulk water molecule, D637, G502, and A635, which may contribute to the stability of this intermediate. In TS2, the H_N-N_ε and the H_N-$O_{2\gamma}$ bonds are 1.47 Å and 1.11 Å, respectively, indicating that the H662 proton H_N is being transferred to ATP γ-phosphate. The proton transfer from H662 to ATP is decoupled from phosphoryl transfer, as the P_γ-$O_{3\beta}$ bond does not change significantly (the P_γ-$O_{3\beta}$ distance is 1.70, 1.71 and 1.65 Å in Min2, TS2, and Min3 respectively), and no P_γ-O_w bond formation is detected (the P_γ-O_w distance is 2.00, 2.01, and 1.94 Å in Min2, TS2, and Min3 respectively). While the H_W-N_ε bond distance varies from 3.05 Å in Min2, through 2.44 Å in TS2, to 3.06 Å in Min3, the H_W-O_W bond is almost unchanged during the transition, suggesting a stepwise proton relay, where H662's donating and accepting proton are well separated. The third step consists of two concerted processes in which the proton transfer of H_W from the lytic water W_L to N_ε of H662 is coupled to the P_γ-O_W bond formation, followed by breaking of the P_γ-$O_{3\beta}$ bond (Scheme 1). As the rate limiting step in the GAC mechanism, the third step goes through a transition state TS3 that is associative in nature and gives rise to an overall barrier height of 22.1 kcal/mol. In TS3, the H_W-O_W bond is elongated to 1.11 Å and the H_W-N_ε bond is shortened to 1.54 Å. The P_γ-$O_{3\beta}$ bond is stretched to 2.02 Å and the P_γ-O_W bond is almost formed at a bond length of 1.72 Å. In the resulting intermediate Min4, the H_W-N_ε bond (1.0 Å) and the P_γ-O_W bond (1.63 Å) are completely formed, but the P_γ-$O_{3\beta}$ bond has not broken yet at this point (1.93 Å). In both TS3 and Min4, P_γ has a trigonal bipyramidal bonding pattern. In Min4, the dihedral angle $O_{1\gamma}$-P_γ-$O_{2\gamma}$-$O_{3\gamma}$ is -163° and the angle $O_{3\beta}$-P_γ-O_W is 166° (not shown in Table S1). Min4 is the most stable state in the whole reaction path (-9.2 kcal/mol). In the last step, cleavage of the P_γ-$O_{3\beta}$ bond leads to the final product complex (Min5), with a P_γ-$O_{3\beta}$ bond of 3.29 Å.

E631 always binds with W_L in the whole process and may serve to stabilize the active site in this mechanism. The length of the hydrogen bond between the sidechain of E631 and W_L ranges from 1.62 to 2.19 Å. The hydrogen bond between E631 and W_L is about 0.5 Å shorter in Min5 than in Min4, which shows that E631 may assist in the P_γ-$O_{3\beta}$ bond breaking. The close interaction between E631 and Pi suggests that E631 may act as a mechanical hinge to the rotation of the helical domain and NBD-TMD communication (Zaitseva *et al. EMBO J* **2006**, *25*, 3432). K508 hydrogen bonds with $O_{1\beta}$ and $O_{2\gamma}$ of ATP simultaneously. The lengths of these two hydrogen bonds are almost equivalent most of the time. In TS3, K508 moves closer to $O_{2\gamma}$ to better stabilize the transition state. During the transition from Min4 to Min5, when Pi moves away from ADP, K508 retains the hydrogen bond with $O_{1\beta}$ of ADP; in contrast, the hydrogen bond between K508 with $O_{2\gamma}$ is weakened, but still within the a reasonable hydrogen bond distance range. In Min5, the H-loop residue H662 forms hydrogen bonds with both $O_{2\gamma}$ and O_W of Pi. Two Ser residues, i.e., the P-loop S504 and the signature loop S607 (from the opposite monomer) form hydrogen bonds with $O_{1\gamma}$ throughout the whole simulation of the reaction. In Min5, the Pi moiety continues to bind to Mg^{2+} ion after hydrolysis, making spontaneous Pi release from the active site less likely. The crystal water W90 forms hydrogen bonds with $O_{2\gamma}$ from Min1 to Min3, and then with N_ε in TS3. The other hydrogen of W90 binds to one of E631 carboxylate oxygens throughout the simulation.

5.2. Geometries and energetics of stationary points for the SAC mechanism

The PES obtained for the SAC mechanism (Figure 2b) also displays a stepwise pattern for ATP hydrolysis. Key geometric parameters and energetics of the stationary points determined for the SAC mechanism are listed in Table S2.

Table S2. Bond distances, dihedral angles, and energies of stationary points in the SAC mechanism (Figure 2b).[a]

	RC1	RC2	Distance (Å)				$O_{1\gamma}$-P_γ-$O_{2\gamma}$-$O_{3\gamma}$ (degrees)	ΔE
			H_W-O_W	H_W-$O_{2\gamma}$	P_γ-$O_{3\beta}$	P_γ-O_W		
Min1	-2.30	-2.10	0.97	3.28	1.66	3.76	148	-6.4
TS1	-2.10	-1.20	0.97	3.08	1.65	2.85	150	7.7
Min2	-1.60	-0.30	0.96	2.55	1.68	1.98	159	0.0
TS2	-0.10	-0.10	1.20	1.31	1.72	1.83	170	32.1
Min3	1.20	0.10	2.15	0.95	1.77	1.68	-173	-0.8
TS3	2.19	0.29	3.14	0.95	1.97	1.68	-162	9.8
Min4	2.29	0.30	3.24	0.95	1.94	1.65	-160	-6.7
TS4	2.49	1.40	3.45	0.96	3.01	1.62	-135	9.1
Min5	2.49	1.80	3.46	0.97	3.40	1.61	-129	7.8

[a]Distances are in Å, dihedral angles in degrees, and energies in kcal/mol.

The SAC reaction route is initiated by formation of a reactant complex (Min2) between W_L and ATP, in which the distance between P_γ and O_W is reduced to 1.98 Å. The second step in SAC is rate limiting and involves two concerted processes that couple proton transfer between the lytic water and $O_{2\gamma}$ of ATP to the P_γ-O_W bond formation, by going through a trigonal bipyramidal transition state (TS2), in which both dihedral angle

$O_{1\gamma}$-P_γ-$O_{2\gamma}$-$O_{3\gamma}$ and the angle $O_{3\beta}$-P_γ-O_W are about 170°. The H_W-O_W and H_W-$O_{2\gamma}$ bonds in TS2 are 1.20 and 1.31 Å, respectively; the P_γ-O_W bond is shortened to 1.83 Å from compared to 1.98 Å in Min2, whereas the P_γ-$O_{3\beta}$ (1.72 Å) is slightly longer than that in Min2 (1.68 Å) and Min1 (1.66 Å). The completion of the proton transfer step in SAC leads to a phosphrane intermediate (Min3) with an energy of -0.8 kcal/mol. In Min3, the newly formed H_w-$O_{2\gamma}$ and P_γ-O_W bonds are 0.95 and 1.68 Å, respectively, indicating that both proton transfer and P_γ-O_W bond formation are completed. The P_γ-$O_{3\beta}$ bond in Min3 is stretched to 1.77 Å, only about 0.1 Å longer than that in Min1 and Min2, implying that the above steps are separated from the P_γ-$O_{3\beta}$ bond scission process next. The third step from Min3 to Min4 corresponds to a structural relaxation of hydrogen bonding interactions involving H662 and E631. This relaxation step is mainly due to mainly due to the rotation of the $O_{2\gamma}$-H_W group about the P_γ-$O_{2\gamma}$ bond. As a result, the $O_{2\gamma}$-H_W bond that originally points to H662 in Min3 is oriented toward the β phosphate in Min4, accompanied by a change of the dihedral angle H_W-$O_{2\gamma}$-P_γ-$O_{3\gamma}$ from -50° to 103°. In Min4, H_W is ready to form a hydrogen bond with the increasingly negatively charged $O_{3\beta}$ atom due to the stretched P_γ-$O_{3\beta}$ bond distance. In addition, there is a hydrogen bond formed between the non-transferred hydrogen on W_L and E631. The resulting intermediate Min4 is the most stable state on the reaction path. The final step in the SAC mechanism is the cleavage of the P_γ-$O_{3\beta}$ bond, resulting in a P_γ-$O_{3\beta}$ bond of 3.40 Å in Min5.

6. Movies.

Movie S1 shows the reaction path identified from Figure 2a for the GAC mechanism, where H662 assists a proton transfer from the lytic water to one of the γ-phosphate oxygens of ATP through a relay. Movie S2 shows the reaction path identified from Figure 2b for the SAC mechanism, where the proton on the lytic water is directly transferred to one of the γ-phosphate oxygens of ATP.

7. Simulations and results of the mechanism of using E361 as a general base and the detailed discussion

To examine the validity of the "catalytic carboxylate" proposal, also referred to as the general base catalysis (GBC) mechanism, we performed additional simulations for or HlyB mediated ATP hydrolysis using E631 as a catalytic base. Two-dimensional potential energy surface (PES) was obtained based on two reaction coordinates RC1 and RC2, where RC1 represents a combined proton transfer reaction coordinate describing proton transfer from lytic water to E631, i.e. $RC1^{GBC}$= O_W-H_W – H_W-$OE2_{E631}$, and RC2 is the reaction coordinate that describes phosphoryl transfer, i.e. $RC2^{GBC}$ = $O_{3\beta}$-P_γ – P_γ-O_w. The 2d-PES of the GBC mechanism is shown in Fig. S1. Key geometries and energetics of stationary points along the reaction path identified for the GBC mechanism (using E631 as a general base) are listed in Table S3. Comparison of energy profiles from GBC, GAC, and SAC is shown in Fig. S2.

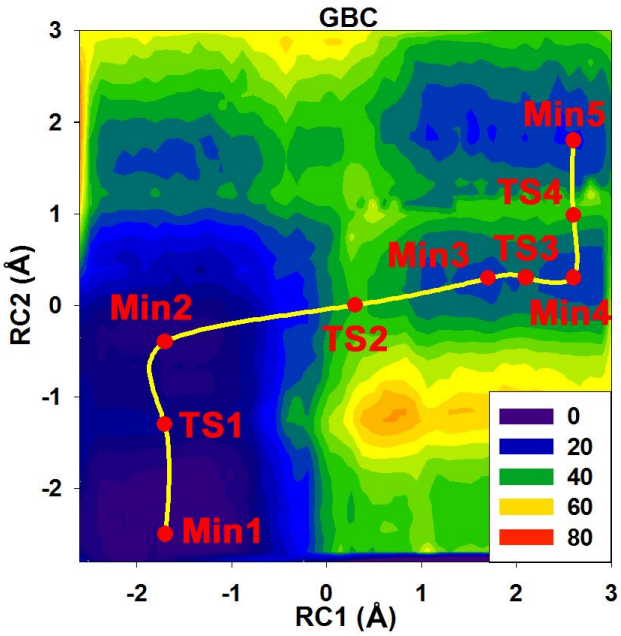

Figure S1. Two-dimensional potential energy surfaces of the general base catalysis (GBC) mechanism where the lytic proton is initially transferred to the general base E631 in the HlyB-NBD mediated ATP-hydrolysis. For the GBC mechanism, the abscissa (RC1) represents a proton-transfer reaction coordinate which is negative as the proton is bonded to the lytic water, and positive as the proton is transferred to the E631 carboxylate oxygen. The ordinate (RC2) is the antisymmetric combination of the $O_{3\beta}$-P_γ and P_γ-O_W bond distances, in describing the phosphoryl transfer reaction during ATP hydrolysis. Distances are in Å, and energies are in kcal/mol.

Table S3. Energies and geometries of stationary points for the GBC mechanism.[a]

	RC1	RC2	Bond distances (Å)				$O_{1\gamma}$-P_γ-$O_{2\gamma}$-$O_{3\gamma}$ (degrees)	ΔE
			H_W-O_W	H_W-OE2	P_γ-$O_{3\beta}$	P_γ-O_W		
Min1	-1.70	-2.50	0.96	2.66	1.66	4.16	150	-5.4
TS1	-1.71	-1.30	0.97	2.67	1.70	3.00	155	6.9
Min2	-1.70	-0.40	0.97	2.67	1.69	2.09	161	0.0
TS2	0.30	0.00	1.40	1.10	1.85	1.84	-179	36.0
Min3	1.70	0.30	2.68	0.98	2.03	1.73	-167	25.5
TS3	2.10	0.30	3.08	0.98	2.03	1.73	-167	26.8
Min4	2.60	0.30	3.58	0.98	2.04	1.74	-166	24.8
TS4	2.60	0.99	3.58	0.98	2.63	1.64	-149	34.0
Min5	2.60	1.80	3.58	0.98	3.46	1.66	-142	20.6

[a]Distances are in Å, dihedral angls in degrees, and energies in kcal/mol.

Similar to GAC and SAC, the first step of the GBC mechanism is associated with the formation of a reactant complex. The second step of in the GBC mechanism is a concerted reaction where the transfer of H_W from O_w of W_L to OE2 of E631 and the P_γ-O_W bond formation occur simultaneously. In the pentacovalent transition state TS2 for this step, H_W-O_W and H_W-OE2 are 1.40 and 1.10 Å, respectively, and the bond lengths of

Electronic Supplementary Material (ESI) for Physical Chemistry Chemical Physics
This journal is © The Owner Societies 2013

P_γ-$O_{3\beta}$ and P_γ-O_W are 1.85 and 1.84 Å, respectively. In Min3, which corresponds to a phosphorane-like intermediate, although Pi has not been fully cleaved from ATP, the bond between P_γ and ADP is weakened as reflected from an elongated P_γ-$O_{3\beta}$ bond of 2.03 Å, meanwhile the P_γ-O_W bond has been formed (1.73 Å). The transition state TS3 mainly corresponds to relaxation involving the protonated E631 after the H_W transfer step; the distance between O_w and E631 increases during the relaxation, indicating weakened hydrogen bonds after E631 is pronated. The transition state TS4 in the last step is associated with breaking the P_γ-$O_{3\beta}$ bond, leading to formation of the final product complex (Min5).

E631 hydrogen bonds with both W_L and the backbone hydrogen of H662 before Min2. From Min2 to TS2, the hydrogen bond between E631 and H662 increases gradually from 2.16 Å to 4.48 Å so that E631 moves closer to W_L to accept H_W. Then this hydrogen bond is weakened and adopts a distance of 2.45 Å in Min3 along with the separation of E631 from W_L. In Min5, this hydrogen bond is shortened to 1.93 Å, lowering the energy of the system. The crystal water W90 stabilizes both $O_{2\gamma}$ and E631 in the initial reactant state structures. After the proton transfer from W_L to E631, the hydrogen bond between W90 and E631 is also weakened. Along the whole reaction process, H662 always maintains hydrogen bond interactions with $O_{2\gamma}$. The crystal water W109 is in the vicinity of W_L but it has no obvious hydrogen bond with W_L prior to TS2. After TS2 is formed, W109 approaches and binds to O_W with a hydrogen bond of 2.31 Å in Min3. The interaction between W109 and O_W is stronger in Min5, showing that in the GAC mechanism, this water helps the P_γ-$O_{3\beta}$ bond breaking instead of E631 as in the GAC and SAC mechanisms.

Figure S2 shows the energy profile of the GBC mechanism (blue) compared with those from GAC (black) and SAC (red). One can see that the GBC mechanism has a barrier height of 36.0 kcal/mol for the rate determining step, corresponding to the proton transfer from the lytic water to carboxylate of E631. This result suggests that the GBC mechanism involving E631 is not an operative one compared to the GAC mechanism in which proton relay through H-loop H662 can be utilized to lower the overall barrier height of ATP hydrolysis by HlyB-NBDs.

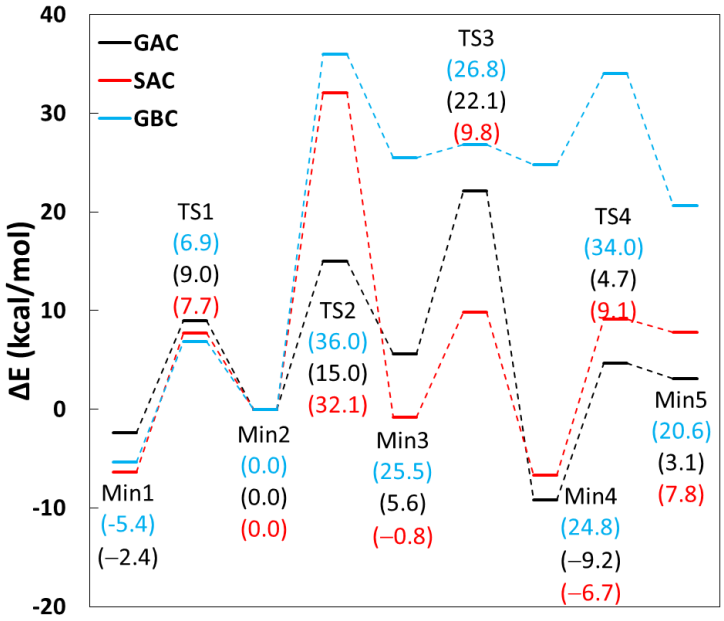

Figure S2. Comparison of energy profiles from the GBC, GAC, and SAC mechanisms.

8. Results of the calculated GAC mechanism by using backward PES scans

In responding to a reviewer's request, we tested the sensitivity of the potential energy surface (PES) scan results by starting the calculation from the hydrolysis products ADP+Pi. For simplicity, we refer to this scan as the "backward" PES scan, in comparison to the "forward" scan, which was carried out from the reactant state ATP+water as presented in the main text. The PES obtained from the backward scan for the GAC mechanism (the operative one) is plotted in Figure S3. The energetics and key geometric parameters for stationary points corresponding to Figure S3 are listed in Table S4. By comparing Figure S3 (backward scan) with Figure 2a (forward scan), we can see that the major features of the GAC mechanism determined by the backward scan, in terms of the topology of the 2-d PES, the locations and natures of the intermediates and transition states, as well as the stationary point energies along the reaction energy profiles, are in good agreement with the results of the forward scan. Quantitative agreement can found by comparing Table S4 (backward scan) and Table S1 (forward scan). For example, the rate-determining barrier heights obtained from the forward and backward scans are 22.1 kcal/mol (forward scan) and 25.1 kcal/mol (backward scan), respectively, and both are associated with TS3 in the two scans. These results confirmed that our computational characterization of the ATP hydrolysis mechanism in HlyB-NBD is insensitive to the direction in which the scan is carried out.

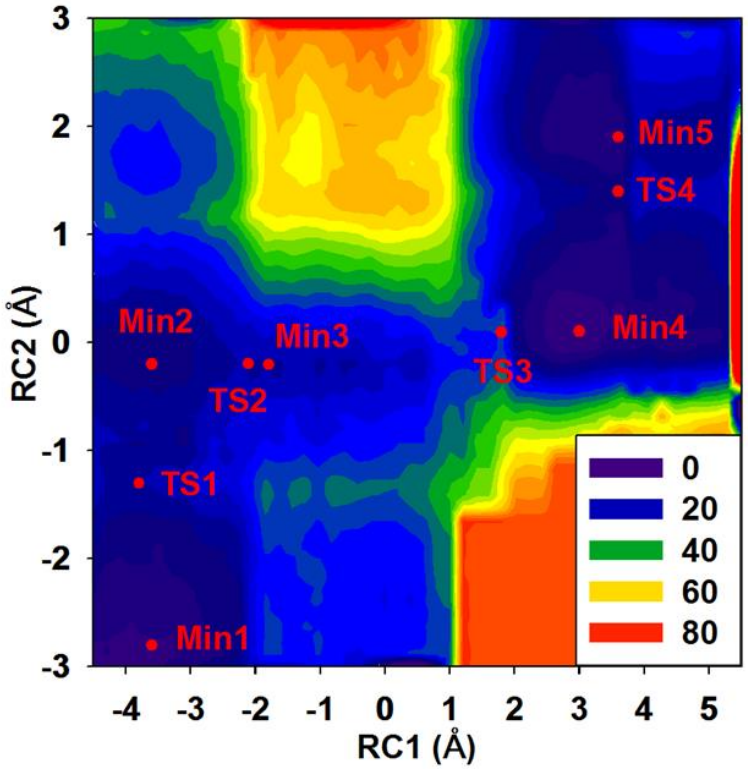

Figure S3. Two-dimensional potential energy surfaces for the general acid catalysis (GAC) mechanism in the HlyB-NBDs mediated ATP-hydrolysis, with PES scan initiated from the product state of ADP + Pi. The abscissa (RC1) represents a proton-relay reaction coordinate which is negative as protons are bonded with lytic water and at N_ε position of H662; zero as the H662 proton is partially transferred to γ-phosphate oxygen $O_{2\gamma}$ of ATP and the lytic water proton is partially transferred to H662, and positive as the proton relay is completed. Energetics and key geometric parameters of stationary points are given in Table S4.

Table S4. Energies and geometries of stationary points for the GAC mechanism, with backward potential energy scan initiated from the ATP hydrolysis product state (see Figures S3 for the two-dimensional potential energy surface).[a]

	RC1	RC2	Δ*E*	H_N-Nε	H_N-$O_{2\gamma}$	H_W-O_W	H_W-Nε	P_γ-$O_{3\beta}$	P_γ-O_W
Min1	-3.60	-2.80	-4.6	0.99	2.24	0.96	3.31	1.67	4.47
TS1	-3.80	-1.30	10.3	1.00	2.22	0.96	3.53	1.68	2.99
Min2	-3.60	-0.20	0.0	1.00	2.05	0.97	3.53	1.75	1.95
TS2	-2.11	-0.20	14.0	1.05	1.70	0.98	2.44	1.83	2.03
Min3	-1.80	-0.20	4.7	2.23	0.96	0.97	4.04	1.67	1.88
TS3	1.80	0.09	25.1	3.43	0.95	1.04	1.73	1.85	1.76
Min4	3.00	0.10	-6.4	2.73	0.95	2.21	0.99	1.78	1.68
TS4	3.60	1.40	2.8	3.57	0.96	1.99	1.00	3.00	1.60
Min5	3.60	1.90	-2.1	3.52	0.96	2.04	1.00	3.49	1.59

[a]Distances are in Å and energies in kcal/mol.

9. Test the system equilibration during the QM/MM MD simulations

In responding to a reviewer, who raised concerns on whether our QM/MM MD simulations was sufficient to equilibrate the system before we initiated the PES scan, we computed root-mean-square-deviations (RMSDs) (Figure S4) on backbone atoms of protein and heavy atoms of ligands with respect to their crystallographic positions during the heating and the subsequent equilibration stages of the QM/MM simulations. As we can see in Figure S4, the RMSD of the system levels off at ~0.9 Å after ~120 ps QM/MM simulations, suggesting that equilibrium has been reached. To confirm the system is sufficiently equilibrated, we also monitored the total energy (Figure S5) of the system along the 160 ps QM/MM MD simulations for heating and equilibration. Figure S5 shows that the total energy of the system reaches a stable value after 50 ps QM/MM MD simulations. Based on Figures S4 and S5, we conclude that the system in our simulations is sufficiently equilibrated.

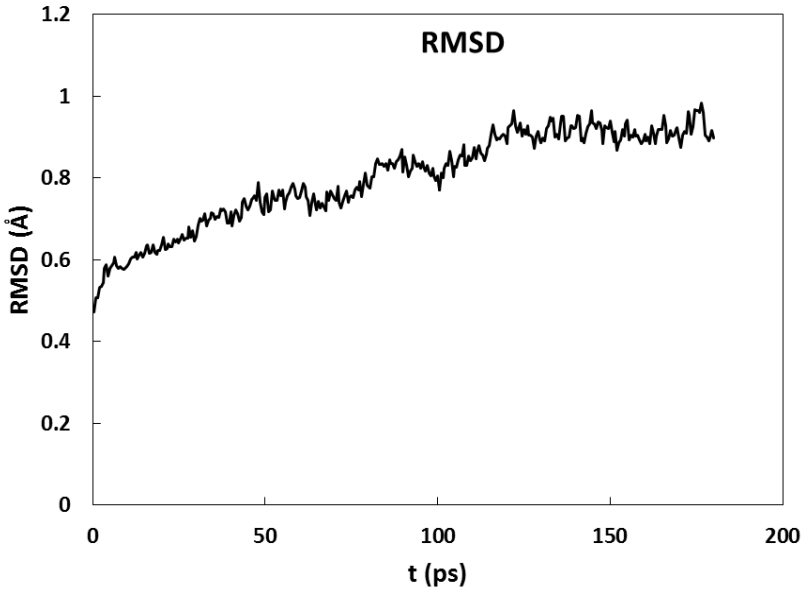

Figure S4. Root-mean-square-deviation (RMSD) of the HlyB system in the heating (60 ps) and equilibration (100 ps) stages of the QM/MM MD simulation. The atoms selected for computing RMSD include protein backbone atoms from dimeric HlyB-NBDs, heavy atoms of the 2 ATP molecules, and the 2 magnesium ions. The reference structure is the minimized crystal structure.

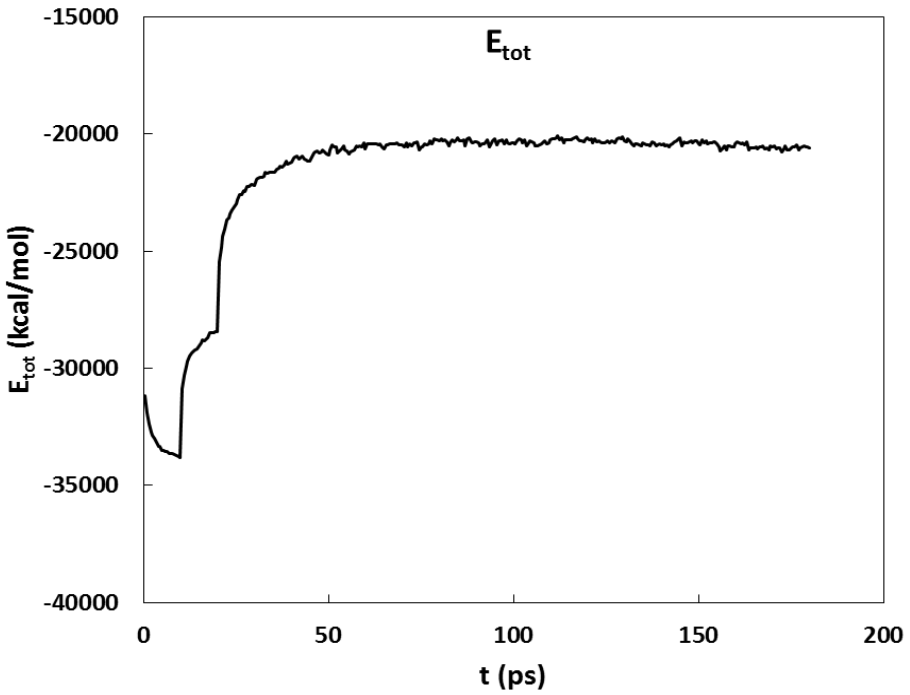

Figure S5. The total energy of the HlyB system in the heating (60 ps) and equilibration (100 ps) stages of the QM/MM MD simulations.

10. Test different non-bond cutoff distances for the QM/MM potential energy scan

In responding to a reviewer's concern on whether the nonbond cutoff distance of 16 Å we used is sufficient to converge the barrier height results, we tested a different non-bonded cutoff value (15 Å) for the operative GAC mechanism (see Figure S6). By comparing Figure S6 (cutoff = 15 Å) with Figure 2a (cutoff = 16 Å) in the text, one can see that the key features of the mechanism displayed by the 2-d potential energy surfaces are essentially the same, which are insensitive to the cutoff distances of the nonbonded interactions. Detailed energies and geometries of stationary points identified by using a cutoff value of 15 Å are given in Table S5. Quantitative agreements of the two cutoff calculations can be seen in the comparison of Table S5 (cutoff =15 Å) and Table S1 (cutoff=16 Å). In particular, we found that the rate determining barrier heights using the two different cutoff values differs less than 1 kcal/mol, i.e., the barrier heights associated with TS3s are 22.1 kcal/mol (cutoff = 15 Å) and 22.0 kcal/mol (cutoff = 16 Å), respectively. These agreements suggest that the use of 16 Å as the nonbond cutoff distance is sufficient and the conclusion drawn upon the calculations presented in the text is not altered with a different cutoff distance; in fact, the comparison of calculations that employ 15 and 16 Å cutoff distances suggest that converged barrier heights can be achieved even with at a shorter cutoff at 15Å.

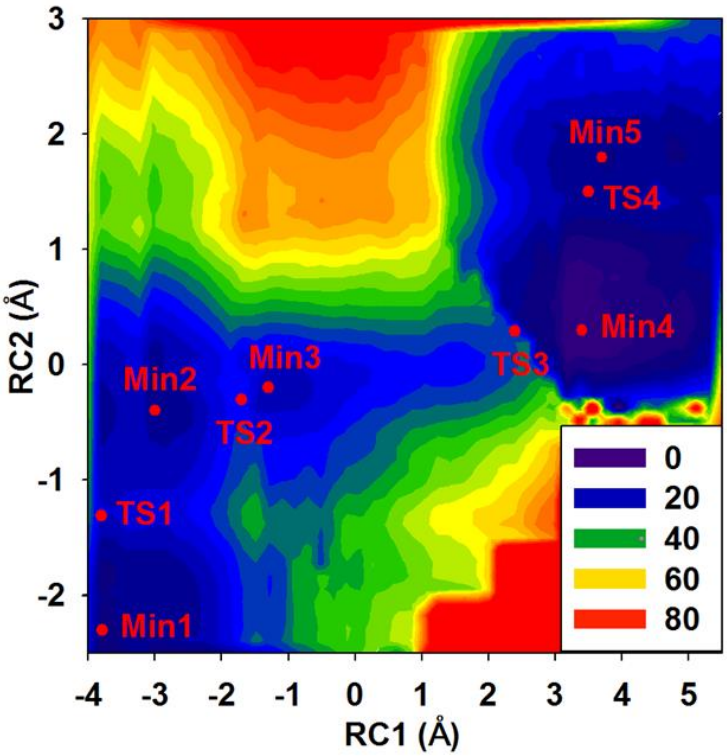

Figure S6. Two-dimensional potential energy surfaces for the general acid catalysis (GAC) mechanism in the HlyB-NBDs mediated ATP-hydrolysis, using a non-bond cutoff value of 15 Å. For comparison, see results in Figure 2a that adopts a cutoff value of 16 Å. The abscissa (RC1) represents a proton-relay reaction coordinate which is negative as protons are bonded with lytic water and at N_ε position of H662; zero as the H662 proton is partially transferred to γ-phosphate oxygen $O_{2\gamma}$ of ATP and the lytic water proton is partially transferred to H662, and positive as the proton relay is completed. Detailed energies and geometries of stationary points associated with Figure S6 can be found in Table S5.

Table S5. Energies and geometries of stationary points for the GAC mechanism, using a nonbond cutoff distance of 15 Å (see Figures S6 for the two-dimensional potential energy surface).[a]

	RC1	RC2	ΔE	H_N-Nε	H_N-$O_{2\gamma}$	H_W-O_W	H_W-Nε	P_γ -$O_{3\beta}$	P_γ -O_W
Min1	-3.79	-2.30	-3.3	1.00	2.03	0.97	3.73	1.67	3.97
TS1	-3.81	-1.31	7.8	1.00	2.03	0.97	3.75	1.73	3.03
Min2	-3.00	-0.40	0.0	1.00	1.99	0.97	2.98	1.68	2.08
TS2	-1.71	-0.30	16.3	1.14	1.40	0.99	2.44	1.71	2.01
Min3	-1.30	-0.20	5.4	1.84	0.98	0.96	3.12	1.72	1.92
TS3	2.40	0.29	21.1	3.86	0.95	1.09	1.60	2.01	1.72
Min4	3.40	0.30	-12.0	3.24	0.95	2.11	1.00	1.93	1.63
TS4	3.50	1.50	1.4	3.41	0.96	2.06	1.00	3.09	1.59
Min5	3.70	1.80	-0.9	3.56	0.96	2.10	1.00	3.38	1.58

[a]Distances are in Å and energies in kcal/mol.